

Seismic Stability of Impoundments

Peter M. Byrne, Ph.D., P. Eng.

Professor Emeritus, Civil Engineering Department, University of British Columbia

Mahmood Seid-Karbasi, M.Sc.

Ph.D. Student, Civil Engineering Department, University of British Columbia

ABSTRACT A number of impoundment have failed or suffered large displacements during past earthquakes. In most cases the damage has occurred as a result of a large drop in the stiffness and strength of soil referred to as liquefaction. Our understanding of liquefaction has increased dramatically in the past 30 years due to: observations from field case histories; extensive laboratory testing of soil elements under cyclic loading; model testing of earth structures under simulated earthquake loading; and development of numerical modeling procedures.

In this paper a dynamic analysis procedure which captures the element data observed in cyclic tests and verified by comparison with model tests and field experience, is applied to Mochikoshi dam. Based on such analyses, implications for design of impoundment structures to resist seismic loading are examined.

Introduction

A number of impoundment type earth structures have failed or suffered large displacements during past earthquakes. In most cases the damage has occurred as a result of a large drop in the stiffness and strength of soil referred to as liquefaction. Classic examples of liquefaction damage are the behaviour of the San Fernando dams during the 1971 San Fernando earthquake, California. The crest of the upper dam moved downstream about 2m, while a flow slide on the upstream side of the lower dam some moments after the severe shaking, removed the crest of the lower dam as shown in Fig 1.

A number of mine tailings impoundment dams have also suffered severe damage during past earthquakes. The best examples here are the Mochikoshi dams in Japan which failed during the 1978 Izu-Ohshim-Kinkai earthquake due to liquefaction induced flow slides resulting in release of the tailings as shown in Fig 2. One dam failed during the shaking, while a second failed 24 hours later.

Our understanding of the seismic behaviour of earth structures has increased dramatically in the past 30 years due to:

- Observations from field case histories,
- Extensive laboratory testing of soil elements under cyclic loading,
- Model testing of earth structures under simulated earthquake loading, and
- Development of numerical modeling procedures.

In this paper a dynamic analysis procedure, which captures the element data observed in cyclic tests and verified by comparison with model tests and field experience, is applied to Mochikoshi dam. Based on such analyses, implications for design of impoundment structures to resist seismic loading are examined.

Soil liquefaction

Seismic liquefaction refers to a sudden loss in stiffness and strength of soil due to cyclic loading effects of an earthquake. The loss arises from a tendency for soil to contract under cyclic loading, and if such contraction is

Fig. 1. Failure of the lower San Fernando dam.



prevented or curtailed by the presence of water in the pores that cannot escape, it leads to a rise in porewater pressure and a resulting drop in effective stress. If the effective stress drops to zero (100% porewater pressure rise), the strength and stiffness also drop to zero and the soil behaves as a heavy liquid. However, unless the soil is very loose it will dilate and regain some stiffness and strength, as it strains. If this strength is sufficient, it will prevent a flow slide from occurring, but may still result in excessive displacements commonly referred to as lateral spreading. In addition, even for level ground condition where there is no possibility of a flow slide and lateral movements may be tolerable, significant settlements may occur due to dissipation of excess porewater pressures during and after the period of strong ground shaking.

Assessment of liquefaction

Liquefaction assessment involves addressing the following concerns:

- Will liquefaction be triggered in significant zones of the soil structure for the design earthquake, and
- If so, could a flow slide occur, and if not,
- Are the displacements tolerable?

These effects can be assessed from state-of-practice total

stress analyses procedures or from state-of-art effective stress analysis procedures.

State-of-Practice procedures address the above 3 concerns with 3 separate analyses; a triggering analysis, a flow slide analysis, and a displacement analysis. The triggering of liquefaction and the concern for a flow slide are addressed in a simplified manner that gives predictions consistent with field experience. However, predictions of displacements are generally based on a simple single-degree-of-freedom Newmark (1965) type analyses, and results are generally not consistent with field experience. Patterns of displacement, which control liner or membrane behaviour, cannot be predicted from such an approach.

In state-of-art effective stress dynamic analyses, porewater pressures are generated in response to the applied earthquake motion and the stiffness and strength of the soil modified accordingly as shaking takes place. More rigorous analyses are based on an elastic plastic stress strain law for the sand skeleton that includes shear induced plastic volumetric strains, and it is these strains under the constraint of the pore fluid stiffness that generate porewater pressure changes. Such an approach allows coupled dynamic stress-flow analyses to be carried out in which both generation and dissipation of porewater pressures and their effects are considered for a specific base motion. The calibration and verification of such models is important and generally involve a 2-step process:

- Simulate and capture the element behaviour as observed in laboratory cyclic tests; simple shear, triaxial, and hollow cylinder;
- Simulate and compare predicted and observed dynamic response for a soil structure.

Ideally, an actual soil structure should be selected. However, even for the best field case histories, such as the San Fernando dams during the 1971 San Fernando earthquake, neither the input motion nor the soil conditions are adequately known. For this reason, verification is currently based on dynamic Centrifuge tests. The first major verification of such models was reported by Arulanandan and Scott, (1993).

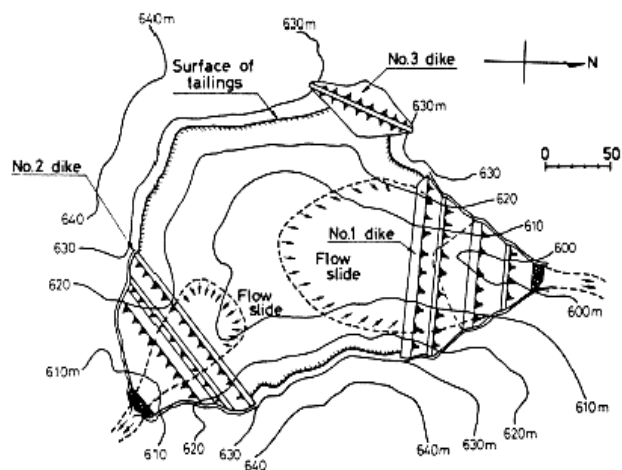
Fully coupled effective stress approaches have been developed by many researchers including Dafalias (1986), Prevost (1989), Zienkiewicz et al. (1990), Byrne et al. (1995), Beaty and Byrne (1998), Elgamal et al. (1999), and Kramer and Arduino (1999). There are a number of journal papers describing comparisons between numerical modeling of liquefaction and comparison with centrifuge tests including Byrne et al. (2003).

In this paper, the UBCSAND model as described by Beaty and Byrne (1998) is applied to Mochikoshi dam.

Mochikoshi tailings dams

The 1978 Izu-Ohshim-Kinkai, Japan earthquakes caused two tailings dams owned by the Mochikoshi gold mining company to fail due to liquefaction of the tailings materials behind the dams. The earthquake comprised of a main shock with magnitude M7 and a large after shock with M5.8. The earthquake was shallow, having a focal depth of about 10 km. Information on the failure of Mochikoshi tailings dams can be found in Marcuson et al. (1979), Okusa and Anma (1980), Okusa et al. (1984), Ishihara (1984), and Jitno and Byrne (1995). A plan view of the tailings dams is shown in Fig. 2.

Fig. 2. Plan of Mochikochi tailings dams (Okusa and Anma 1980).



Ishihara (1984) estimated the peak ground acceleration at the dam sites was about 0.15 to 0.25g at the ground surface. Dam No. 1 failed during the main shaking. Dam No. 2, failed about 24 hours after the main shock. The delayed failure of the No. 2 dam was postulated to be due to upward movement of the phreatic surface resulting from liquefaction of the tailings deposits behind the dam (Ishihara 1984).

The geotechnical information obtained at the dam sites, in addition to the reported failure mechanism of both dams, makes this case one of the several unique case histories of dam failure caused by earthquake-induced liquefaction. It has been used to check the validity of procedures proposed for predicting the deformation behavior of earth-structures under earthquake loading by researchers (e.g. Jitno and Byrne 1995, Olson 2001). In this paper, the deformation behavior of the Mochikoshi tailings dam No. 1 is examined using a dynamic coupled effective stress-flow analysis.

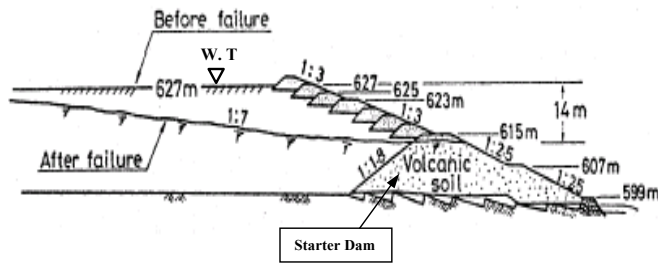
Earthquake effects on dam No.1

The cross-section of the dam is presented in Fig. 3 and shows geometry before and after the failure. The tailings impoundment was used to store gold mine waste, and the dam was built using an upstream construction method with a starter dam comprised of Volcanic soil. The impoundment had been in operation since 1964.

Dam No. 1 had a maximum height of 28 m, a crest length of 73m, and a crest width of 5 m. The water table at the time of earthquake was approximately 3m below the slope surface and in the pond at top surface. The tailings dam failed catastrophically during the main shaking and resulted in flow of tailings down the valley over a distance of about 800 m (Ishihara 1984).

The guardian of the dam witnessed this catastrophic event. According to him, as reported by Ishihara (1984), "within about 10 seconds of the shaking, the frontal wall of the dam swelled causing excessive vertical movements at the crest...". At this time, the tailings presumably had liquefied.

Fig. 3. Cross-section of dam No. 1 (Ishihara 1984).



Geotechnical conditions of the dam

The tailings materials consisted of 3 to 7 cm thick layers of silt with a plasticity index of 10, and a non-plastic sandy silt with an average fine content 80% (finer than sieve #200). The average standard penetration resistance of the tailings reported in geotechnical drillings conducted about 3 weeks after the failure was about zero to 2 above a depth of 15 m and about 3 to 7 at greater depths. Ishihara (1984) noted that this low N value might have been due to soil remolding caused by liquefaction during the shaking. As demonstrated by Byrne & Beaty (1997) for the flow failure at the Mufulira Mine in Zambia in 1970, mixing of sandy silt soils significantly reduces its strength leading to further strength and stiffness loss after liquefaction was triggered. It is likely therefore that the original blow counts of the tailings at Mochikoshi were somewhat higher. It was assumed that the average N value was 2. The equivalent $(N_1)_{60-cs}$ corrected for overburden and fines content was estimated to be 6 based on Seed (1985) and Youd et al. (2001).

The results of static triaxial tests on undisturbed tailings indicated a zero cohesion and a friction angle ϕ' varying between 30 and 39 degrees. The liquid limit of tailings varied between 27 to 31%, whereas the moisture content ranged from 36 to 37%. A water content greater than the liquid limit indicates that the tailings would be very susceptible to strength loss as they sheared. The permeability of the tailings, based on in-situ and laboratory tests, was 10^{-4} and 10^{-7} (cm/sec) in horizontal and vertical directions, respectively. The much lower vertical permeability was estimated by Ishihara (1984) and arises from the stratified nature of the tailings. The void ratio of the tailings was 0.98 and 1.0 and specific gravity was 2.72 and 2.74, respectively, for the sandy silt and silt portions of the tailings (Ishihara 1984).

The starter dam itself was placed and compacted by bulldozers and consisted of a mixture of weathered tuffs and volcanic ash obtained from the borrow pit adjacent to the dam. It comprised a mix of gravel, sand and silt and had a 65% fines content. Its unit weight ranged between 14 and 19 kN/m³. The natural moisture content ranged between 30% to 60%, and void ratio 1.1 to 2.6. Triaxial tests on undisturbed samples resulted in $C'=25$ kPa and $\phi' = 35$ degrees, and the permeability was reported to be 10^{-4} (cm/sec). The average N value was reported to be about 5. This material did not liquefy during the earthquake and was not tested for liquefaction resistance. The above properties were reported by Ishihara (1984).

Numerical modeling

Dynamic analysis of the Mochikoshi dam No.1 was carried out using the UBCSAND constitutive model for the tailings materials. It is based on the elastic-plastic stress strain model proposed by Byrne et al. (1995), and has been further developed and extended by Puebla et al. (1997), and Beaty and Byrne (1998). It is an incremental elastic-plastic model in which the yield loci are lines of constant stress ratio. The flow rule relating the plastic strain increment directions is non-associated and leads to a plastic potential defined in terms of dilation angle. The model is implemented in the commercial computer code FLAC (Fast Lagrangian analysis of Continua, ITASCA, 2000).

The appropriate parameters for the model can be obtained directly from cyclic testing of undisturbed samples from the site, or indirectly from field experience with similar soils during past earthquakes. The common practice is the indirect approach with liquefaction response expressed in terms of penetration resistance, and this approach was used here. The UBCSAND model has been calibrated to reproduce the Youd et al. (2001) triggering chart which in turn is based on field experience during past earthquakes and is expressed in terms of Standard Penetration Test resistance value, $N_{1(60)}$. The model properties to obtain such agreement are therefore expressed in terms of $N_{1(60)}$. It has also been calibrated with cyclic simple shear test data for Nevada sand as well as Fraser river sand and predicts both triggering as well as post triggering response in close agreement with the data as shown in Fig. 4. The agreement is obtained by selecting an $N_{1(60)}$ to give the best fit to data. In this way an $N_{1(60)}$ value equivalent to the known relative density, D_r , of the laboratory test sample is obtained.

The model grid together with material types representing different grid parts of the dam in the analysis is illustrated in Fig.5.

In the first stage static analysis the Mohr-Coulomb model with stress-dependent materials properties was utilized for all parts. The soil was treated as equivalent elastic and isotropic using secant shear (G) and bulk (B) moduli that vary with stress level as follows:

$$[1] \quad G = k_g \cdot Pa \cdot \left(\frac{\sigma'_m}{Pa} \right)^n$$

$$[2] \quad B = k_b \cdot Pa \cdot \left(\frac{\sigma'_m}{Pa} \right)^m$$

In which k_g and k_b are shear and bulk modulus numbers, n and m are modulus exponents, σ'_m is the mean effective stress, and P_a is atmospheric pressure. The materials properties are listed in Table 1 and were based on test data and experience with similar soils.

Subsequently, the UBCSAND model was applied to the slime material, while the Mohr-Coulomb model was used for other parts deemed not to liquefy. The model parameters were determined based on $N_{1(60)cs} = 6$ for the slime materials.

No time histories of acceleration at or near the site were recorded for this earthquake. For this reason a history from the San Fernando M6.5 earthquake measured

Fig. 4. Comparison of predicted and measured response, a) excess pore pressure, b) stress path, c) No. of cycles.

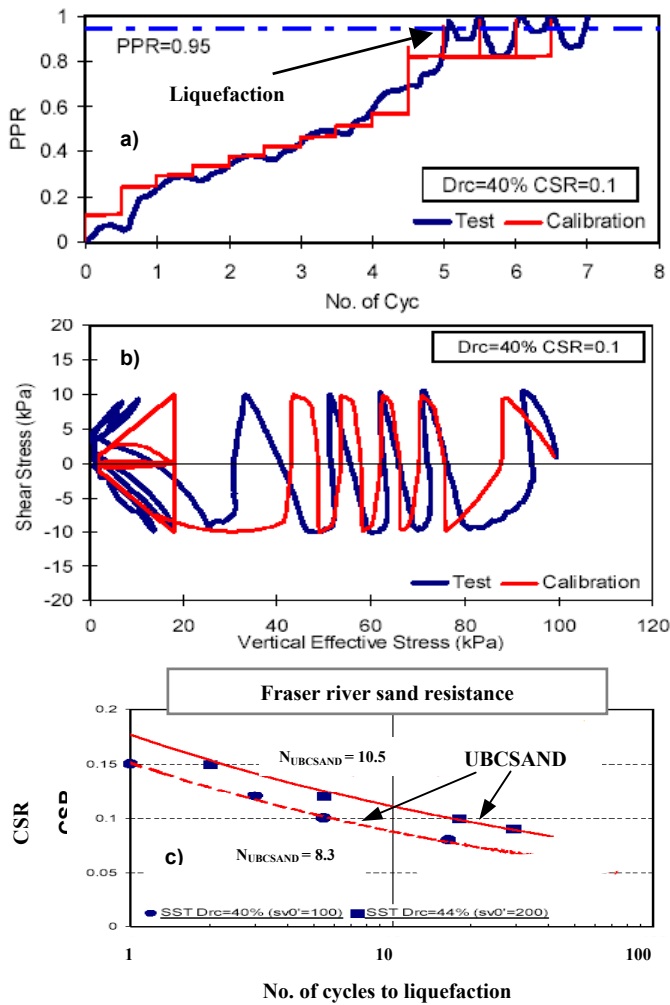
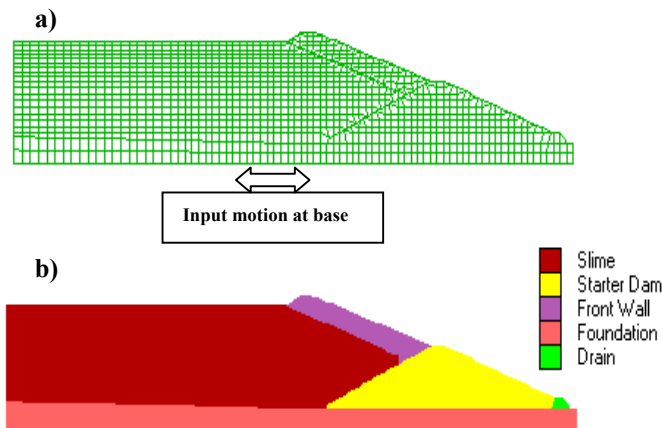
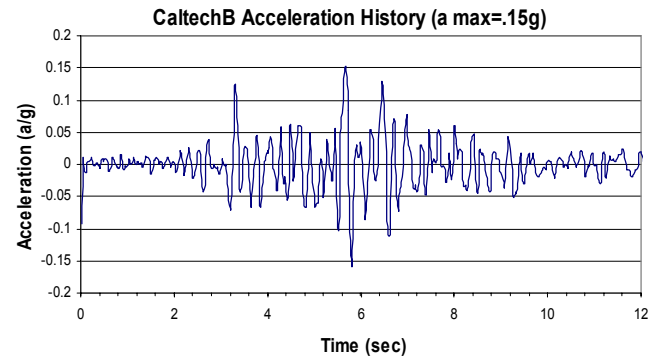


Fig. 5. Dam model (a) Grid, (b) types of materials.



at the Caltech B Station (California Institute of Technology) and normalized to $a_{max} = 0.15g$ was applied at the base of the model, and is as shown in Fig. 6.

Fig. 6. Input earthquake acceleration record.



This earthquake has a shallow focal depth similar to Izu-Ohshim-Kinkai earthquake, but a lower magnitude, M6.5 vs. M7, and is thought to be reasonably appropriate.

Results of the analyses

The response of the dam during the earthquake in terms of acceleration, excess pore pressure (U_e), excess pore pressure ratio (R_u) and deformations is presented in Figs. 7 to 12. Fig. 9 shows the relative positions of locations selected for illustrations here.

Fig. 7 shows the predicted acceleration time histories for specific points at different depths (see Figs. 9 for locations). It indicates that the input motion is amplified to some extent at depth, e.g. A1 and then de-amplified in the upper tailings at A2 and A3 due to the occurrence of liquefaction.

Predicted excess pore pressures as a function of time are shown in Fig. 8. It may be seen that the pore pressures rise rapidly in the time 3 to 8 Secs. corresponding to the period of strong shaking and then level off. Significantly higher excess pore pressures are generated at depth, indicating upward flow of water.

Predicted excess pore pressure ratios R_u are shown in Figs. 10 and 11, where R_u is the ratio of the excess pore pressure to the initial effective stress. $R_u = 1$ represents a condition of 100% pore pressure ratio and complete liquefaction. Fig. 10 represents condition under level ground conditions back from the crest of the dam. It may be seen that near the surface the pore pressures rises to $R_u = 1$ corresponding to 100% pore pressure rise and a fully liquefied state. At increasing depths, predicted R_u values are somewhat lower ($R_u = 0.7$).

Beneath the sloping face of the dam, the predicted maximum R_u values as illustrated in Fig. 11 are significantly lower, in the range 0.4 to 0.8 as opposed to 0.7 to 1.0. This is consistent with the results of dynamic centrifuge model tests where significantly lower R_u values are observed beneath sloping as compared to level ground (Taboda and Dobry, 1995).

The predicted deformations of the dam at the end of earthquake shaking are illustrated in Fig. 12 and Fig. 13 in terms of displacement vectors and distorted grid and indicate large displacement of about 5m. The tailings are predicted to liquefy and move up and over the starter dam resulting in upward movement of the front wall consistent with the failure mode observed by the guardian at the time of the failure.

Table 1. Materials properties used in the analysis.

Soil	kg	n	kb	m	ϕ ($^{\circ}$)	C (kPa)	γ_t (kN/m ³)	Perm. (cm/sec)
Front wall	110	0.5	330	0.5	35.0	25.0	15.7	1e-4
Starter Dam	126	0.5	378	0.5	35.0	25.0	15.7	1e-4
Drain	150	0.5	450	0.5	45.0	0.0	19.0	1e-2
Found.	150	0.5	450	0.5	35.0	25.0	15.7	1e-3
Slime*	96	0.5	289	0.5	34.0	0.0	18.4	kx = 7.1e-4 ky = 7.1e-7

*) UBCSAND model was applied to this material with $N_{1(60)cs} = 6$ and $\phi_{cv} = 33.0$.

Fig. 7. Acceleration time history at different depths.

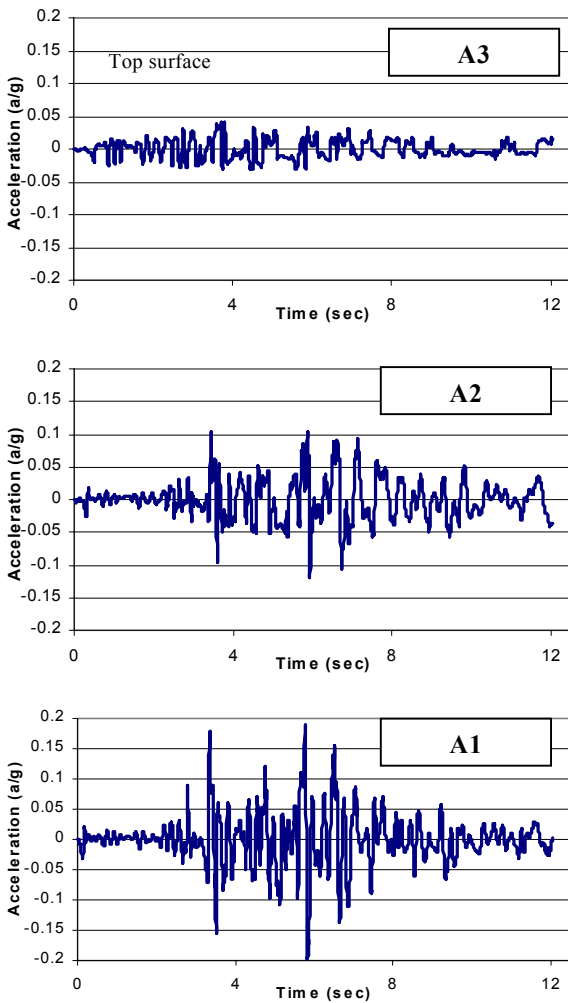


Fig. 8. Excess pore pressure at different depths.

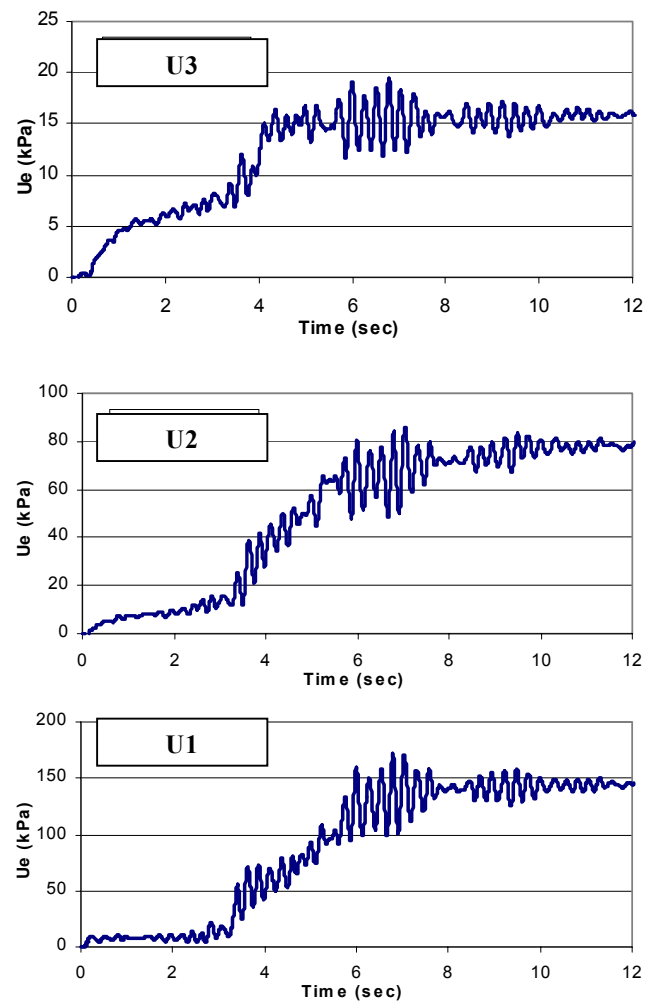


Fig. 9. Relative positions of locations for acceleration and excess pore pressure recording in analysis.

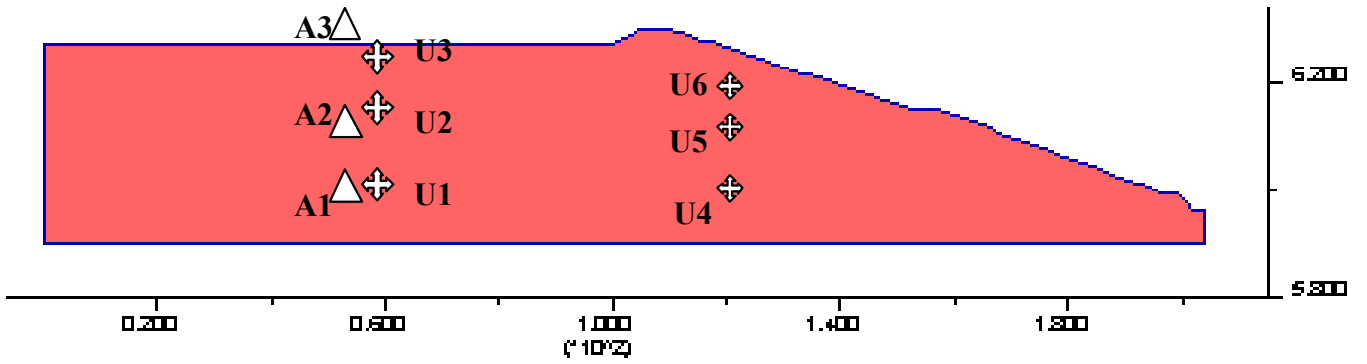
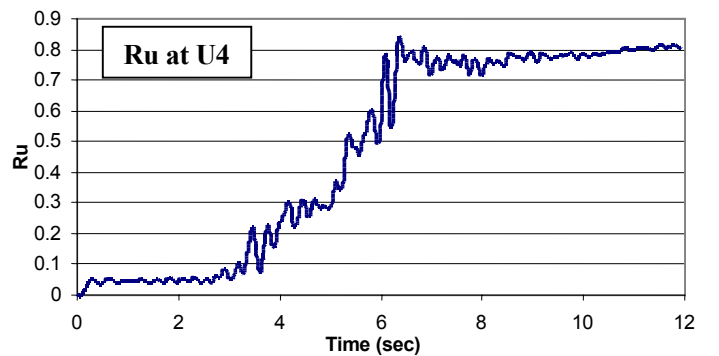
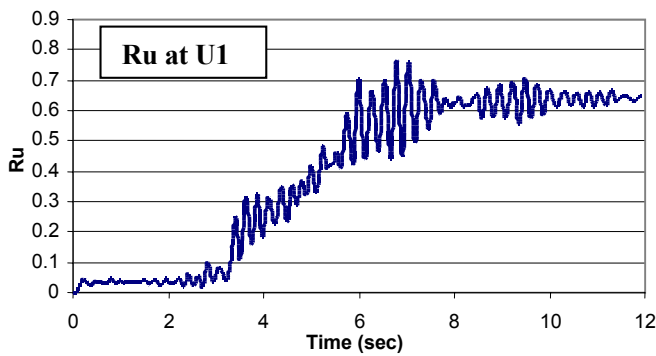
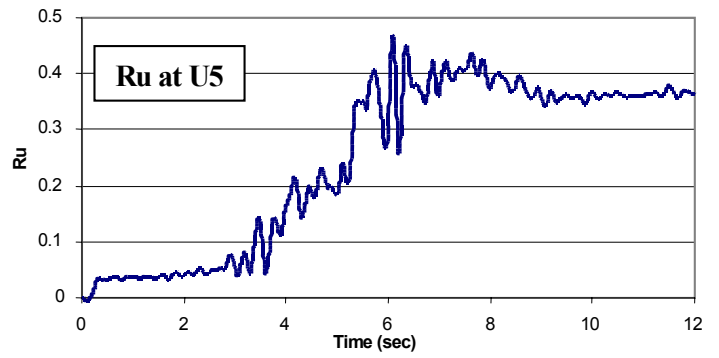
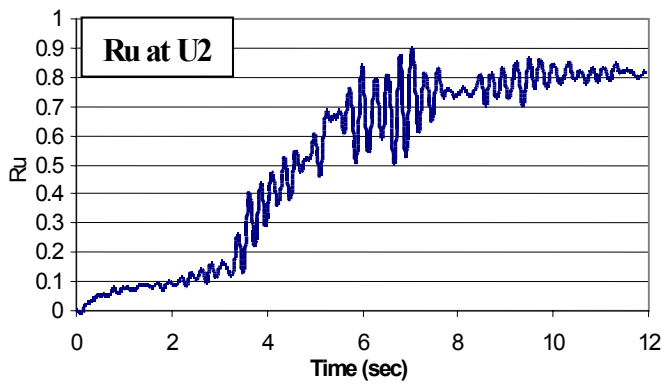
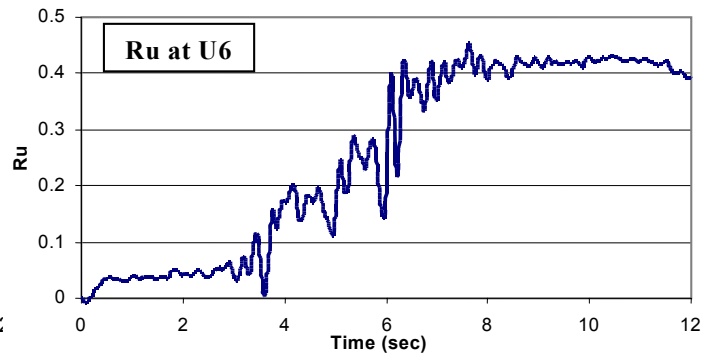
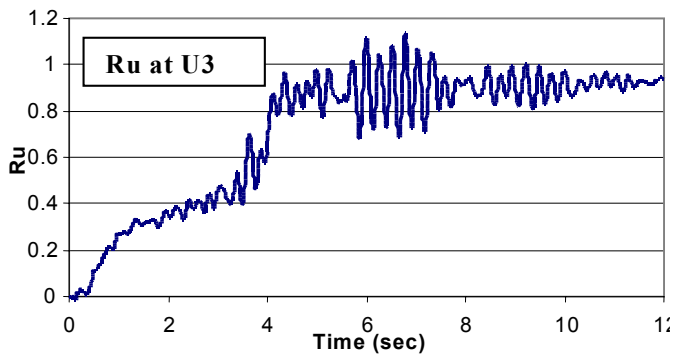


Fig. 10. Pore pressure ratio (R_u) at different depths

Fig. 11. Pore pressure ratio (R_u) beneath the slope



Lessons learned

Lessons learned from field experience, laboratory tests, and analyses are:

- The seismic failure of dam No.1 at the Mochikoshi impoundment likely occurred due to liquefaction of the tailings. The presence of layers of plastic silt having a natural water content in excess of the liquid limit likely caused a further strength loss resulting in flow of the tailings once significant displacements occurred.
- The Mochikoshi dam could have been stabilized by a free draining buttress fill or by a stabilized column as shown in Figs. 14a and 14b.
- Horizontal layers of low permeability, barrier layers, impede vertical drainage of excess porewater pressure and can greatly reduce stability as they may cause a water bubble to form at the base of the layer during or after the shaking as observed by Kokusku et al. (2000) in shaking table tests and shown in Fig. 15. Such layers may have caused the delayed failures at the Lower San Fernando dam and at the Mochikoshi No. 2 Dike.
- The bubble effect can be prevented by vertical drains that penetrate the barrier layers as illustrated in Fig. 16. The design of these drains can be assessed from dynamic coupled flow effective stress analyses.
- Liquefaction induced displacements can be curtailed by a stabilizing soil column having a width at least equal to the depth of liquefaction as shown schematically in Fig. 17.
- The dimensions and location of remediation measures can be optimized from dynamic analyses. Stabilization can be achieved by densification, drainage or bonding of soil particles to prevent liquefaction.

Conclusion

A number of impoundment dams have failed during past earthquakes as a result of soil liquefaction. Plastic sandy silt layers may have water contents greater than their liquid limit, in which case they may lose more strength when significant displacements are induced by seismic loading. The failure of dam No. 1 at the Mochikoshi impoundment likely occurred in this manner.

Laboratory model testing suggests that clean loose sands are unlikely to suffer a flow slide, because, although they can be triggered to liquefy, their undrained strengths are generally adequate for stability unless they are very loose. However, if the sands contain low permeability silt layers that impede drainage, water bubbles and complete loss of strength can occur. The delayed failure of dyke No.2 at the Mochikoshi impoundment as well as the delayed failure of the Lower San Fernando dam may well have occurred in this manner.

Fig. 12. Displacement vectors due to earthquake.

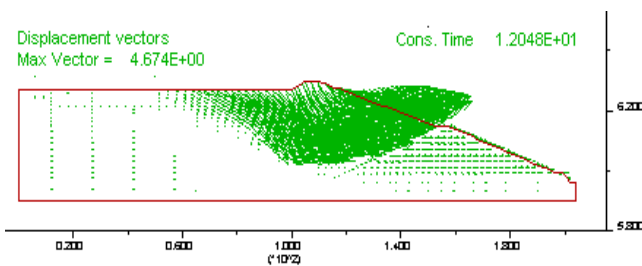


Fig. 13. Distorted grid (3 times magnified for clarity).

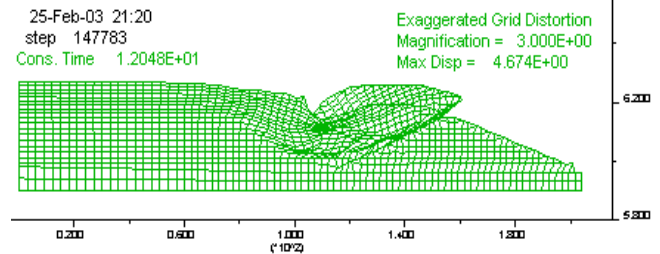


Fig. 14. Remediation of Mochikoshi dam, a) buttress fill, b) stabilizing column

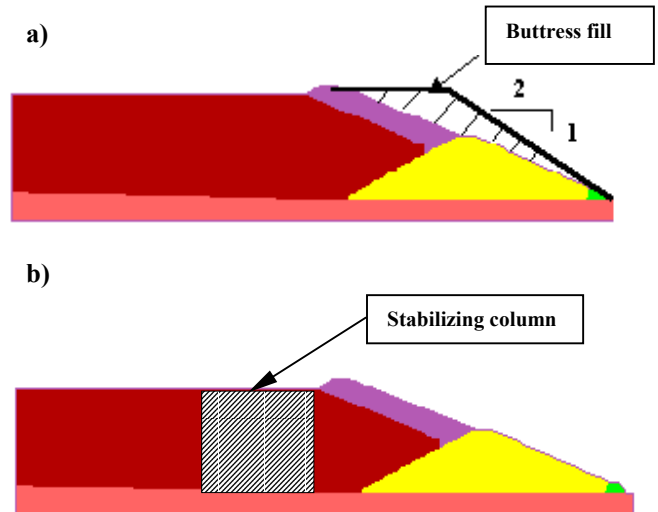


Fig. 15. Water bubble under barrier layer due to shaking.

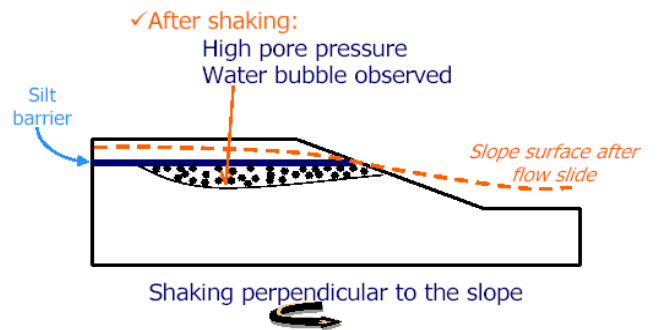


Fig. 16. Drains to curtail bubble effects

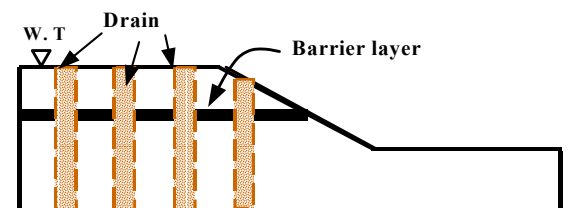
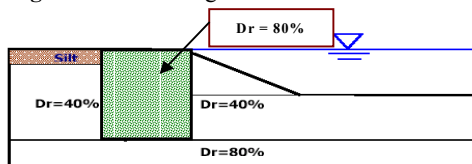


Fig. 17. Stabilizing soil column



References:

- Arulanandan, K., and Scott, R.F. 1993. Verification of numerical procedures for the analysis of soil liquefaction problems. Proceedings of the International Conference on the Verification of Numerical Procedures for the Analysis of Soil Liquefaction Problems, Vols. 1 and 2, Balkema, Rotterdam, the Netherlands.
- Beatty, M. H. and Byrne, P. M. 1998. An Effective stress model for predicting liquefaction behavior of sand, *In Proceedings of Specialty Conf., Geotechnical Earthquake Engg. and Soil Dynamics III*, Seattle, ASCE GSP No. 75, Edited by Dakoulas, M. and Holtz, R.D., V. 1, pp. 766-777.
- Byrne, P. M., and Beatty, M. H. 1997. Post-liquefaction shear strength of granular soils: theoretical/conceptual issues. *In Proceedings, Workshop on Post-Liquefaction Shear Strength of Granular Soils*, Urbana-Champaign, Illinois, April 17-18, 1997, pp. 16-45.
- Byrne, P. M., Park, S., Beatty, M., Sharp, M., Gonzales, L., and Abdoun, T. 2003. Numerical modeling of liquefaction and comparison with centrifuge tests. Submitted to Canadian Geotechnical Journal.
- Byrne, P.M., Phillips, R., and Zang, Y. 1995. Centrifuge tests and analysis of CANLEX field event, 48th Canadian Geotechnical Conference, Vancouver, British Columbia.
- Byrne, P.M., Roy, D., Campanella, R.G., and Hughes, J. 1995. Predicting liquefaction response of granular soils from pressuremeter tests. ASCE National Convention, San Diego, Oct. 23-27, ASCE, Geotechnical Special Publication 56, pp. 122-135.
- Dafalias, Y.F. 1986. Bounding surface plasticity. I: mathematical foundation and the concept of hypoplasticity. *Journal of Engineering Mechanics*, ASCE, **112** (9), pp. 966-987.
- Elgamal, A.-W., Parra, E., Yang, Z, Dobry, R., and Zeghal M. 1999. Liquefaction constitutive model. *In Proc., Physics and Mechanics of Soil Liquefaction Symposium*, Balkema, Rotterdam, The Netherlands, pp. 269-279.
- Ishihara, K. 1984. Post-earthquake failure of a tailings dam due to liquefaction of the pond deposit. *In Proc., Inter. Conf. on Case Histories in Geotechnical Engineering*, Rolla, Missouri, May 6-11, Vol. 3, pp. 1129-1143.
- ITASCA, 2000. Fast Lagrangian analysis of continua (FLAC), Version 4, User's Guide. Itasca Consulting Group, Inc., Thrasher Square East, 708 South Third Street, Suite 310, Minneapolis, Minnesota.
- Jitno, H. and Byrne, P.M. 1995. Predicted and observed liquefaction response of Mochikoshi tailings dam. *In Proc., the First Inter. Conf., Earthquake Geotechnical Engineering*, Tokyo, Nov. 14-16, 1995, Vol. 2, pp. 1085-1090.
- Kokusho, T., and Kojima, T., Nonaka, N., 2000. Emergence of water film in liquefied sand and its role in lateral flow. *In Proc., the 12th World Conf., Earthquake Engg., Auckland, New Zealand, Jan., 30-Feb., 4, 2000*, Paper No. 946.
- Kramer, S., and Arduino, P. 1999. Constitutive modeling of cyclic mobility and implications for site response. *In Proceedings of the 2nd International Conference on Earthquake Geotechnical Engineering*, Balkema, Rotterdam, The Netherlands, pp. 1029-1034.
- Marcuson, W.F., III, Ballard, R.F., Jr., and Ledbetter, R.H. 1979. Liquefaction failure of tailings dams resulting from the Near Izu Oshima earthquake, 14 and 15 January, 1978. *In Proc. 6th Pan-American Conf. on Soil Mechanics and Foundation Engineering*, Lima Peru, Vol. 2, pp. 69-80.
- Newmark, N. M., 1965. Effects of Earthquakes on Dams and Embankments. *J., Geotechnique*, **15**(2), pp. 139-160.
- Olson, S. M., 2001. Liquefaction analysis of level and sloping ground using field case histories and penetration resistance. Ph. D. Thesis, University of Illinois, Urbana-Champaign.
- Okusa, S. and Anma, S. 1980. Slope failures and tailings dam damage in the 1978 Izu- Ohshima-Kinkai earthquake. *Journal of Engineering Geology*, **16**, pp. 195-224.
- Okusa, S., Anma, S., and Maikuma, M. 1984. The propagation of liquefaction pressure and delayed failure of a tailings dam dike in the 1978 Izu-Oshima-Kinkai earthquake. *In Proc., 8th World Conf. on Earthquake Engineering*, July 21-28, San Francisco, CA, Vol. 1, pp. 389-396.
- Prevost, J.H. 1989. DYNA1D: A computer program for nonlinear site response analysis. Technical Report No. NCEER-89-0025, National Center for Earthquake Engineering Research, SUNY at Buffalo, NY.
- Puebla, H., Byrne, P. M., and Phillips, R., 1997. Analysis of CANLEX liquefaction embankment: prototype and centrifuge models. *Canadian Geotechnical Journal*, **34**, pp. 641-654.
- Puebla, H., 1999. A constitutive model for sand analysis of the CANLEX embankment. Ph.D. thesis, University of British Columbia, Vancouver, Canada.
- Seed, H. B., Tokimatsu, K., Harder, L. F., and Chung, R. M. 1985. The influence of SPT procedures in soil liquefaction resistance evaluations. *J. Geotech. Engrg.*, ASCE, **111**(12), pp. 1425-1445.
- Taboada-Urtuzuastegui V.M. and Dobry R. 1995. Centrifuge modeling of earthquake-induced lateral spreading in sand. *Journal of Geotechnical Engineering*, ASCE, **124**(12), pp. 1195-206.
- Youd, T. L., Idriss, I. M., Andrus, R., Arango, I., Castro, G., Christian, J., Dobry, J., Finn, L., Harder Jr., L., Hynes, H. M., Ishihara, K., Koester, J., Liao, S. S., Marcuson III, W. F., Martin, G., Mitchell, J. K., Moriwaki, Y., Power, M. S., Robertson, P. K., Seed, R. B., and Stokoe II, K. H., 2001. Liquefaction Resistance of Soils: Summary Report from the 1996 NCEER and 1998 NCEER/NSF Workshops on Evaluation of Liquefaction Resistance of Soils, *J., Geotechnical and Geoenvironmental Engg.*, ASCE, **127**(10), pp. 817-833.
- Zienkiewicz, O.C., Chan, A.H.C., Pastor, M., Paul, D.K., and Shiomi, T. 1990. Static and dynamic behavior of soils: a rational approach to quantitative solutions. Part I: fully saturated problems. *In Proceeding, Research Society London*, A429, pp. 285-309.